Int. J. Radiation Oncology Biol. Phys., Vol. 75, No. 4, pp. 1155–1161, 2009

0360-3016/09/$–see front matter

ELSEVIER

doi:10.1016/j.ijrobp.2008.12.083

CLINICAL INVESTIGATION **Brain**

PEDIATRIC CRANIOSPINAL AXIS IRRADIATION WITH HELICAL TOMOTHERAPY: PATIENT OUTCOME AND LACK OF ACUTE PULMONARY TOXICITY

JOSÉ PEÑAGARÍCANO, M.D.,* EDUARDO MOROS, PH.D.,* PETER CORRY, PH.D.,* ROBERT SAYLORS, M.D.,†‡ AND VANEERAT RATANATHARATHORN, M.D.*

Departments of *Radiation Oncology and †Pediatric Hematology-Oncology, University of Arkansas for Medical Sciences College of Medicine, Little Rock, AR; and ‡Department of Pediatric Hematology-Oncology, Arkansas Children's Hospital, Little Rock, AR

Purpose: To present the patient outcomes and risk of symptomatic acute radiation pneumonitis (ARP) in 18 pediatric patients treated with helical tomotherapy to their craniospinal axis for a variety of neoplasms.
Methods and Materials: A total of 18 patients received craniospinal axis irradiation with helical tomotherapy. The median age was 12 years (range, 2.5–21). The follow-up range was 3–48 months (median, 16.5). Of the 18 patients, 15 received chemotherapy in the neoadjuvant, adjuvant, or concomitant setting. Chemotherapy was tailored to the particular histologic diagnosis; 10 of 18 patients underwent surgical removal of the gross primary tumor. The patients were followed and evaluated for ARP starting at 3–6 months after completion of craniospinal axis irradiation. ARP was graded using the Common Toxicity Criteria, version 3.
Results: At the last follow-up visit, 14, 2, and 2 patients were alive without disease, alive with disease, and dead of disease, respectively. The cause-specific survival rate was 89% (16 of 18), disease-free survival rate was 78% (14 of 18), and overall survival rate was 89% (16 of 18). No patient had treatment failure at the cribriform plate. No patient developed symptoms of ARP.
Conclusion: Craniospinal axis irradiation using helical tomotherapy yielded encouraging patient outcomes and acute toxicity profiles. Although large volumes of the lung received low radiation doses, no patient developed symptoms of ARP during the follow-up period. © 2009 Elsevier Inc.

Pediatric cancer, craniospinal irradiation, pulmonary toxicity, helical tomotherapy.

INTRODUCTION

Novel technology for radiotherapy for large and complex targets is an attractive proposition. This holds true for conventional craniospinal axis (CSA) irradiation (CSAI) in which a matched and marching junction between the cranial and spinal fields is required to minimize the risk of radiation myelopathy, with patients usually treated in the prone position. However, it is cumbersome to deliver general anesthesia with the patient in this position. Moreover, proper technique is needed to avoid treatment failure at the cribriform plate. We expected that technologies such as helical tomotherapy (HT), would simplify treatment delivery to complex targets such as the CSA and minimize treatment technique-associated risks.

Our evaluation of intensity-modulated radiotherapy for CSAI began in 2002 (1, 2). A feasibility analysis of CSAI with HT was published in 2005 (3), with later publications showing that in CSAI with HT the excess dose to the healthy tissue can be redistributed, and, in turn, the total integral dose to the patient can be lower than in conventional external beam delivery (4, 5). Our clinical experience (6) has shown that HT can generate acceptable clinical treatment plans with reasonable beam-on times with patients in the supine position. A potential drawback in the use of HT is the delivery of small doses to large volumes of tissue (5). This is of particular concern in sensitive structures such as the lungs. In HT for CSAI, the entire lung volume receives small radiation doses, which could theoretically injure the lungs and result in acute radiation pneumonitis (ARP) (7, 8).

The lung dose–volume parameters to use in this patient population for optimization of the treatment plans are unknown. The available parameters used for the planning of lung cancer and Hodgkin's lymphoma treatment might provide a guide. However, we suspect that such parameters might not be applicable to pediatric patients who need treatment to

Reprint requests to: José Peñagarícano, M.D., Department of Radiation Oncology, University of Arkansas for Medical Sciences College of Medicine, 4301 W. Markham, #771, Little Rock, AR 72205. Tel: (501) 686-7100; Fax: (501) 686-7285; E-mail: penagaricanojosea@uams.edu

Conflict of interest: none.

Acknowledgments—We would like to acknowledge research support from the Central Arkansas Radiation Therapy Institute (CARTI). We also would like to thank the Medical Dosimetry group at UAMS-CARTI for their support in de-identified data management and skillful treatment planning.

Received Oct 23, 2008, and in revised form Dec 16, 2008. Accepted for publication Dec 24, 2008.

Table 1. Radiotherapy Oncology Group and Common Toxicity Criteria grading of radiation-induced pneumonitis

Grade	RTOG definition	CTC v.3 definition
1	Mild symptoms of dry cough or dyspnea on exertion	Asymptomatic; radiographic findings only
2	Persistent cough requiring narcotic, antitussive agents; dyspnea with minimal effort but not at rest	Symptomatic; not interfering with ADL
3	Severe cough unresponsive to narcotic antitussive agent or dyspnea at rest/ clinical or radiologic evidence of acute pneumonitis/intermittent oxygen or steroids might be required	Symptomatic; interfering with ADL; patient requires oxygen
4	Severe respiratory insufficiency/continuous oxygen or assisted ventilation	Life-threatening; ventilatory support indicated
5	Not applicable	Death

Abbreviations: RTOG = Radiation Therapy Oncology Group; CTC v.3 = Common Toxicity Criteria, version 3; ADL = activities of daily living.

the CSA, because these parameters could be confounded by pre-existing medical conditions not present in the pediatric population.

Acute radiation pneumonitis occurs 3–6 months after the end of a radiotherapy course. The diagnosis is determined from the clinical symptoms and radiographic findings, with or without pulmonary function test abnormalities. However, the diagnosis can be uncertain in ≤28% of patients because of confounding co-existing medical conditions (9). ARP subsides with time but can progress to pulmonary fibrosis. Another potential risk is underdosing the cribriform plate during CSAI with HT, as presented by Bauman *et al.* (10). These investigators commented on the consequence of selecting a wide-fan beam, which results in less resolution for dose shaping around the cribriform plate. This in turn could result in a potential treatment failure in this area.

In the present study, we evaluated the treatment outcomes and incidence of symptomatic (Common Toxicity Criteria [CTC], version 3, Grade 2 or greater; Table 1) ARP in 18 pediatric patients treated to the CSA with HT, as well as the risk of cribriform failures.

METHODS AND MATERIALS

Helical tomotherapy Hi-ART system

Helical tomotherapy is based on the combined principles of a linear accelerator and a computed tomography (CT) scanner (11–13). The HT fan beam, with a maximal width and length at the isocenter of 5 and 40 cm, respectively, is modulated by a binary multileaf collimator. Patients are positioned on the treatment couch that moves through a rotating ring gantry. HT can acquire megavoltage CT (MVCT) images with clinically useful image quality and resolution for image-guided radiotherapy. Alignment of the treatment planning CT scan with the MVCT scan permits daily repositioning of the patient to account for interfraction changes in the patient's anatomy or position (14–16). Because the planning target volume in CSAI is large in the longitudinal axis, we performed MVCT sampling (17) as a routine procedure. In this process, MVCT scans of the head, chest, and pelvis are obtained and fused automatically to the planning CT image using the bony anatomy and the regions of interest are outlined. This process not only reduces the setup time, but also minimizes the imaging radiation exposure to the patient. The exposure is also affected by the selected resolution of the MVCT images, which were obtained in the normal scanning mode. The automated fusion was verified both manually and visually in the axial,

Table 2. Patient characteristics

Pt. No.	Age (y)	Diagnosis	Resection of primary tumor before RT	Chemotherapy	Total dose (Gy)/dose per fraction (Gy)*
1	11	Medulloblastoma	Yes, complete	Yes	23.4/1.8
2	9	Relapsed acute leukemia	No	Yes	15.0/1.5
3	15	Pineoblastoma	Yes, complete	Yes	36.0/1.8
4	16	Pure germinoma	No	No	25.2/1.8
5	18	Ependymoma	No	No	40.0/2.0
6	15	Astrocytoma	No	Yes	36.0/1.8
7	15	Rhabdoid	Yes, complete	Yes	36.0/1.8
8	5	Medulloblastoma	No, recurrent disease	Yes	36.0/1.8
9	2.5	Medulloblastoma	No, recurrent disease	Yes	34.2/1.8
10	8	Gliomatosis	No	Yes	36.0/1.8
11	6	PNET	Yes, complete	Yes	36.0/1.8
12	21	Medulloblastoma	Yes, complete	No	36.0/1.8
13	7	Pineal mixed germ cell tumor	Yes, complete	Yes	36.0/1.8
14	13	Pineoblastoma	Yes, complete	Yes	36.0/1.8
15	16	PNET	No	Yes	36.0/1.8
16	5	Pineoblastoma	Yes, complete	Yes	36.0/1.8
17	4	Pineal mixed germ cell tumor	Yes, complete	Yes	36.0/1.8
18	16	Pineoblastoma	Yes, complete	Yes	36.0/1.8

Abbreviations: Pt. No. = patient number; RT = radiotherapy; PNET = primitive neuroectodermal tumor.
* Prescription set so 95% of planning target volume would receive specified dose.

sagittal, and coronal planes. The shifts in coordinates determined by this procedure were then used for patient positioning.

Patients and regions of interest

The patient characteristics are listed in Table 2. The median age was 12 years (range, 2.5–21). Of the 18 patients, 15 received chemotherapy in the neoadjuvant, adjuvant, or concomitant setting. Chemotherapy was tailored to the histologic diagnosis. No patient had previously undergone radiotherapy, and 10 of the 18 patients had undergone gross surgical removal of the primary tumor. The reasons for not undergoing resection of the primary tumor varied: 1 patient was diagnosed with isolated central nervous system relapse of acute lymphocytic leukemia, 1 had a pure central nervous system germinoma, 1 had a sacral ependymoma, 1 had an intracranial astrocytoma with diffuse spinal metastasis, 2 were treated for tumor recurrence, 1 had gliomatosis cerebri with spinal cord involvement, and 1 had a primitive neuroectodermal tumor with diffuse central nervous system metastasis. All patients received radiotherapy to the CSA (Table 2). When indicated, patients received a radiation boost to the residual disease in the brain, posterior fossa, or spine or to the brain tumor bed, posterior fossa tumor bed, or gross spinal tumors as seen on pretherapy magnetic resonance imaging. The boost dose, if any, was dependent on the diagnosis. At the conclusion of treatment, the patients were followed on a regular basis with physical examinations and imaging studies.

The University of Arkansas for Medical Sciences institutional review board approved this study (Record 81244).

Definition of regions of interest

All patients underwent CT simulation (Brilliance model, Philips Healthcare [formerly, Philips Medical Systems], Andover, MA) and 5-mm-thick slices and spacing were obtained. Vacuum cradles and thermoplastic masks were used for immobilization in the supine position. The need for anesthesia was evaluated on a patient-by-patient basis. The organs at risk and targets were contoured into the CT simulation data set using the Pinnacle^3 Planning Station (Philips Healthcare, versions 7.6c or greater). The biologic target in the brain for CSAI is the whole brain, cerebellum, subarachnoid space, and cribriform plate (clinical target volume-brain). This clinical target volume-brain is much larger than the gross tumor volume-brain, which is usually the postoperative tumor bed and any associated residual tumor. To define the planning target volume (PTV)-brain, the reminder of the entire cranial contents was used as a margin to the clinical target volume-brain, in addition to the inner surfaces of the skull and the base of the skull. The biologic target for the spine is the spinal cord and its thecal sac from the foramen magnum to the end of the thecal sac as seen on magnetic resonance imaging of the spine (gross tumor volume-spine). Because we desired a homogeneous dose to the entire spine, the PTV-spine was selected as the entire spine from the foramen magnum to, usually, the bottom of the sacroiliac joint. Finally, the PTV-brain and PTV-spine were combined to create the treatment PTV.

HT-CSAI treatment planning

The CT simulation data set and region of interest files were transferred to the HT planning station using the Digital Imaging and Communications in Medicine-radiotherapy protocol. To decrease the computational time and memory requirements of the HT treatment planning system, the CT simulation data sets were downsampled from 256 × 256 to 128 × 128 pixels. The optimization was guided using several user-selected parameters, which have been previously reported (18). The HT planning system uses an iterative inverse treatment planning optimization algorithm based on least-squares minimization. The dose computation was determined using the superposition/convolution method (19). The prescription for each patient is noted in Table 2. To the best of our knowledge, no published data are available on how to define the lung's objective for this particular treatment scenario and delivery technique. Hence, we used the values published for treatment of lung cancer and Hodgkin's lymphoma in adults (Table 3) as a guide (20–24). The optimization objectives to the lungs were defined to limit the mean dose, percentage of lung volume receiving ≥20 Gy (V_{20}), and V_{30} to no more than 16 Gy, 25%, and 22%, respectively. No attempt was made during the optimization process to limit the V_{10}, V_{13}, and V_{15}. Once a plan was finalized and approved for treatment, several dose–volume parameters were extracted from the treatment planning system: the V_{10}, V_{13}, V_{15}, V_{20}, and V_{30}, mean lung dose (MLD), normalized total mean lung dose (NTD_{mean}) at 2 Gy/fraction accounting for late effects calculated using the linear-quadratic equation (25), and total lung volume.

Table 3. Range values predicting 10–20% risk of radiation pneumonitis in patients treated for lung cancer or Hodgkin's lymphoma

Investigator	Parameter	Value
Schallenkamp *et al.* (20)	V_{10} (%)*	31–43
Schallenkamp *et al.* (20)	V_{13} (%)*	28–39
Schallenkamp *et al.* (20)	V_{15} (%)*	26–46
Schallenkamp *et al.* (20); Tsujino *et al.* (22)	V_{20} (%)*	20–29
Fay *et al.* (21)	V_{30} (%)†	<22
Koh *et al.* (23)	MLD (Gy)†	<14–16
Kwa *et al.* (24)	NTD_{mean} (Gy)†	<16–20

Abbreviations: V_{xx} = percentage of lung volume receiving ≥xx Gy; MLD = mean lung dose; NTD_{mean} = normalized total dose of mean dose; other abbreviations as in Table 1.

* 10–20% risk of Grade 2 or greater radiation pneumonitis (CTC v.3)

† Risk of RTOG Grade 2 or greater acute radiation pneumonitis.

ARP grading

Acute radiation pneumonitis was graded using the CTC, version 3 (Table 1). All patients were evaluated clinically starting 3–6 months after CSAI completion for any signs or symptoms of symptomatic (Grade 2 or greater) ARP. The patients were also assessed for symptoms and signs of ARP at every follow-up visit until the window for ARP had passed (6 months after CSAI completion).

RESULTS

Patient outcome

The follow-up range was 3–48 months (median, 16.5). At the last follow-up visit, 14, 2, and 2 patients were alive without disease, alive with disease, and dead of disease, respectively (Table 4). The cause-specific survival rate was 89% (16 of 18), disease-free survival rate was 78% (14 of 18), and overall survival rate was 89% (16 of 18).

Acute toxicity

Acute toxicities were graded using the CTC, version 3 (Table 5). The most common acute toxicity grade of any kind was Grade 2. The most common acute toxicity was

Table 4. Patient outcomes

Pt. No.	Status	Follow-up (mo)	Cribriform failure	Symptomatic ARP*
1	AWOD	48	No	No
2	AWOD	43	No	No
3	AWOD	30	No	No
4	AWOD	28	No	No
5	AWD	39	No	No
6	DOD†	10	No	No
7	AWOD	19	No	No
8	AWOD	17	No	No
9	AWOD	30	No	No
10	AWD	16	No	No
11	AWOD	17	No	No
12	AWOD	14	No	No
13	AWOD	9	No	No
14	AWOD	9	No	No
15	AWOD	9	No	No
16	DOD†	3	No	No
17	AWOD	8	No	No
18	AWOD	8	No	No

Abbreviations: Pt. No. = patient number; ARP = acute radiation pneumonitis; AWOD = alive without disease; AWD = alive with disease; DOD = dead of disease.

* Determined by clinical examination 3–6 months after craniospinal axis irradiation.

† Disease progression.

Table 5. Acute (CTC v.3) toxicities other than acute radiation pneumonitis

	Grade					
Pt. No.	Skin	Nausea	Vomiting	Esophagitis	Back pain	Weight loss
1		1				2
2	1					
3		1	1			2
4				1		
5						
6						1
7		2	2	2		2
8		2	2	1		2
9	2					2
10	1					1
11		2				1
12		2				1
13		2	2			2
14		2	2		2	
15				2		1
16	1	1				2
17		1				2
18					3	1

Abbreviations: CTC v.3 = Common Toxicity Criteria, version 3; Pt. No. = patient number.

weight loss ($n = 14$) followed by nausea ($n = 10$). Patients experiencing nausea and vomiting received antinausea/antiemetic medication, with resolution of symptoms. The greatest acute toxicity seen was Grade 3 low back pain in 1 patient. No Grade 4 or 5 toxicities developed.

Lack of symptomatic ARP

Figure 1 shows the average V_{10}, V_{13}, V_{15}, V_{20}, and V_{30} values, and Fig. 2 shows the average MLD and NTD_{mean} for all patients obtained from the tomotherapy planning station. No patient developed symptomatic ARP. Because the optimization objectives for the lungs were defined to limit V_{20} and V_{30}, and the MLD was kept at or less than the desired value by additional manipulation of the optimization objectives, none of the values obtained for the dose–volume or dose parameters exceeded our goal. However, the V_{10}, V_{13}, and V_{15} varied from patient to patient. The V_{10} and V_{13} ranged from 10.3% to 83.5% (median, 57.3%) and from 3.9% to 50.8% (median, 34.5%), respectively. The V_{15}, V_{20}, V_{30}, MLD, and NTD_{mean} were within the limits (Table 3). Of the 18 patients, 15 and 6 had a risk greater than 20% for CTC, version 3, Grade 2 ARP as determined by the V_{10} and V_{13}, respectively. None of these patients developed symptomatic ARP.

Cribriform plate

No cribriform plate failures were seen (Table 4).

DISCUSSION

We have previously shown that (*1*) CSAI with HT is feasible with patients in the supine position, thus facilitating the administration of general anesthesia when needed (3); (*2*) the integral dose with HT is not necessarily larger than that with three-dimensional conformal radiotherapy (3D-CRT) or conventional techniques (4, 5); and (*3*) HT can generate acceptable clinical treatment plans with reasonable beam-on times using a jaw width of 5.0 cm, pitch of 0.287, and modulation factor of 2.0 (6). The general concerns in treating patients with CSAI include the potential underdosing of the cribriform plate, as seen with conventional treatment, and the potentially high risk of symptomatic ARP owing to irradiation of large lung volumes. In the present study, we have reported the patient outcomes, potential rate of symptomatic ARP, and cribriform failure rates using HT.

Because our group of 18 patients presented with a variety of diagnoses, a comparison of our tumor control results with the published data stratified by the specific diagnoses was not possible. With a median follow-up of 16.5 months, our patients had a cause-specific survival rate of 89%, disease-free survival rate of 78%, and overall survival rate of 89%, with no failures at the cribriform plate. Our cribriform failure rate compared favorably with those for medulloblastoma found in published studies with reported rates of 2.5–11% (26–28). Most of these failures were attributed to poor planning technique.

Laboratory data have identified two distinct pathogenic processes in the development of radiation pneumonitis (RP), and these have an equal effect on pathologic features (29). The first is the vascular damage induced by lower doses. This type of damage showed a large capacity for recovery with minimal long-term structural or functional consequences but with early functional loss when large volumes of the lung have received low radiation doses. In contrast,

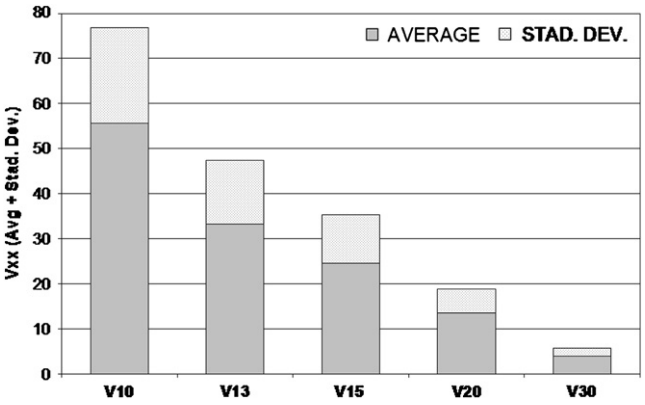

Fig. 1. Average V_{xx} in 18 pediatric patients treated to craniospinal axis with helical tomotherapy. V_{xx} = volume parameter describing volume of lungs (in percentages) receiving xx Gy; Avg = average; Stad Dev = standard deviation.

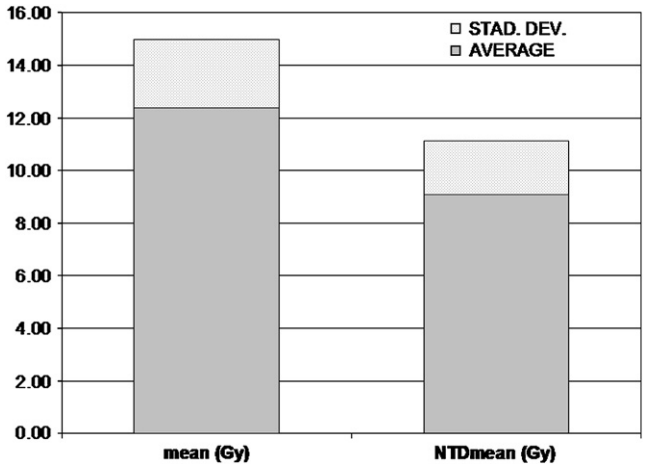

Fig. 2. Average mean lung dose and lung normalized total dose mean average in 18 pediatric patients treated to craniospinal axis with helical tomotherapy.

the parenchymal inflammation produced by higher doses almost always ended in morphologically and clinically expressed fibrosis, but small-volume irradiation did not lead to substantial function loss at any postirradiation interval despite the very high doses and severe parenchymal injury.

Several dose–volume metrics (MLD or V_x) have been used to predict the risk of ARP in the irradiated lung. Claude *et al.* (30) evaluated in a prospective fashion the relationship of both clinical and dosimetric prognostic factors with RP in patients with non–small-cell lung cancer treated with 3D-CRT. That study concluded that the mean lung dose, V_{20}, V_{30}, and patient age were all predictive of the development of Grade 1 or greater RP risk measured using the late effects Normal Tissue–Subjective, Objective, Management, Analytic scale. However, these quantities do not reflect the entire complexity of the dose–volume relationship (31). Laboratory data from the irradiated rat lung have suggested that the volume of the lung irradiated to small doses might be the most significant prognostic factor for radiation-induced loss of pulmonary function (32). Novakova-Jiresova *et al.* (29) also investigated the dose–volume dependence of respiratory function in a rat model. Their conclusion corroborated the findings of Semenenko *et al.* (32). That is, a low dose scattered over a large lung volume causes more early toxicity than an extreme dose confined to a small volume. These conclusions raise concerns with the use of intensity-modulated beams to reduce the MLD, because the volume of lung receiving low radiation is expected to be larger (33, 34). In addition, it seems that a decrease in the MLD to minimize the risk of RP might not be sufficient to overcome the effects of irradiating a large volume of the lung with small doses (35). Hence, it would be prudent to minimize exposure of large volumes of normal lung during the optimization process, but this could be difficult to do. Others have studied the serum cytokine levels as prognostic factors in the development of RP. Arpin *et al.* (36) investigated variations in the circulating serum levels of interleukin-6 and -10 and tumor necrosis factor-α during 3D-CRT in patients with non–small-cell lung cancer and their correlation with the occurrence of RP. Their study concluded that early variations in serum interleukin-6 and -10 levels during 3D-CRT were significantly associated with the risk of RP.

In our group of 18 patients treated with HT and evaluable for ARP, 11 patients had $\geq$50% of the lung volume that received $\geq$10 Gy. In the other 7 patients, the V_{10} was <50%. None of these 18 patients developed symptoms of ARP during the evaluation window of 3–6 months after CSAI completion or at any time during the follow-up period. We agree with Semenenko *et al.* (32) in that the potential hazard of large lung volume irradiation with intensity-modulated beams warrants additional investigation, preferably through clinical trials. The use of dose–volume parameters from the lung cancer and Hodgkin's disease population might overpredict the risk of ARP in this group of CSAI pediatric patients. Usually lung cancer patients have underlying pulmonary conditions that might predispose them to pneumonitis, such as emphysema and chronic obstructive pulmonary disease. The same holds true for the Hodgkin's disease population, because in many cases, these patients are exposed to pulmonary toxic drugs such as bleomycin. The underlying disease processes might account for the differences observed in our population and the predictions based on these published data in lung cancer and Hodgkin's disease patients. Different dose–volume parameters are needed to predict the risks of ARP in this specific group of pediatric patients.

The limitations of the present study were the relatively short median follow-up time of 16.5 months. As such, no firm conclusions could be made in terms of late toxicity to the lungs in this group of patients. Also, we did not perform a prospective evaluation using pulmonary function tests to correlate the loss of lung function with the potential onset of clinical ARP.

CONCLUSIONS

We have updated our experience with HT for CSAI. No patient in this group developed symptomatic ARP even though

most of them received small doses to large lung volumes. The threshold values of V_{20}, V_{30}, and MLD from lung cancer and Hodgkin's disease series provided safe dose–volume parameters against the development of symptomatic RP. The ultimate thresholds of these and other parameters for the development of ARP in pediatric patients treated to the CSA remain unknown. We encourage more studies examine the dose–volume parameters in pediatric CSAI patients and the predicted risk of ARP. In our group of patients, HT for CSAI yielded acceptable and encouraging overall survival, cause-specific survival, and disease-free survival. Appropriate coverage of the cribriform plate is important because failures in this area have been reported with poor CSAI technique. In our study, no such failures occurred. As we reported previously, the treatment of the CSA using HT provides some important advantages. The most salient ones are that no cranial to spinal field radiation matching is needed, that the treatment of patients in the supine position is possible, facilitating patient comfort and anesthesia when needed, and lack of ARP and cribriform plate failures.

REFERENCES

1. Papanikolaou N, Peñagarícano J, Yan Y, *et al*. A feasibility study of IMRT for cranio-spinal treatment. *Radiother Oncol* 2002;64(Suppl. 1):S97.
2. Papanikolaou N, Yan Y, Peñagarícano J, *et al*. Application of IMRT for the treatment of medulloblastoma. *Med Phys* 2002; 29:1215.
3. Peñagarícano J, Papanikolaou N, Yan Y, *et al*. Feasibility of cranio-spinal axis radiation with the Hi-Art tomotherapy system. *Radiother Oncol* 2005;76:72–78.
4. Peñagarícano J, Shi C, Ratanatharathorn V. Evaluation of integral dose in cranio-spinal axis (CSA) irradiation with conventional and helical delivery. *Technol Cancer Res Treat* 2005;4: 683–690.
5. Peñagarícano J, Shi C, Ratanatharathorn V. Integral dose in pediatric craniospinal irradiation with the helical tomotherapy Hi-ART System. In: Mehta M, Paliwal BR, Bentzen S, editors. Physical, chemical & biological targeting in radiation oncology. Proceedings from the 7th International Conference on Dose, Time and Fractionation. Madison, WI: Medical Physics Publishing; 2005. p. 92–93.
6. Peñagarícano J, Yan Y, Corry P, *et al*. Retrospective evaluation of pediatric cranio-spinal axis irradiation plans with the Hi-Art tomotherapy system. *Technol Cancer Res Treat* 2007;6: 355–360.
7. De Neve W, De Wagter C. Lethal pneumonitis in a phase I study of chemotherapy and IMRT for NSCLC: The need to investigate the accuracy of dose computations. *Radiother Oncol* 2005;75:246–247.
8. Holloway CL, Robinson D, Murray B. Results of a phase I study to dose escalate using intensity modulated radiotherapy guided by combined PET/CT imaging with induction chemotherapy for patients with non-small cell lung cancer. *Radiother Oncol* 2004; 73:285–287.
9. Kocak Z, Evans ES, Zhou SM, *et al*. Challenges in defining radiation pneumonitis in patients with lung cancer. *Int J Radiat Oncol Biol Phys* 2005;62:635–638.
10. Bauman G, Yartsev S, Coad T, *et al*. Helical tomotherapy for craniospinal radiation. *Br J Radiol* 2005;78:542–548.
11. Mackie TR, Balog J, Ruchala K, *et al*. Tomotherapy. *Semin Radiat Oncol* 1999;9:108–117.
12. Mackie TR, Holmes T, Swerdlof S. Tomotherapy: A new concept for the delivery of dynamic conformal radiotherapy. *Med Phys* 1993;20:1709–1719.
13. Yang JN, Mackie TR, Reckwerdt P, *et al*. An investigation of tomotherapy beam delivery. *Med Phys* 1997;24: 425–436.
14. Kapatoes JM, Olivera GH, Reckwerdt P, *et al*. Delivery verification in sequential and helical tomotherapy. *Phys Med Biol* 1999;44:1815–1841.
15. Kapatoes JM, Ruchala K, Similowitz JB, *et al*. A feasible method for clinical delivery verification and dose reconstruction in tomotherapy. *Med Phys* 2001;28:528–542.
16. Peñagarícano J, Papanikolaou N. Intensity-modulated radiotherapy for carcinoma of the head and neck. *Curr Oncol Rep* 2003;5:131–139.
17. Hui SK, Kapatoes J, Fowler J, *et al*. Feasibility study of helical tomotherapy for total body or total marrow irradiation. *Med Phys* 2005;32:3214–3224.
18. Grigorov G, Kron T, Wong E, *et al*. Optimization of helical tomotherapy treatment plans for prostate cancer. *Phys Med Biol* 2003;48:1933–1943.
19. Shepard DM, Olivera GH, Reckwerdt PJ, *et al*. Iterative approaches to dose optimization in tomotherapy. *Phys Med Biol* 2000;45:69–90.
20. Schallenkamp JM, Miller RC, Brinkman DH, *et al*. Incidence of radiation pneumonitis after thoracic irradiation: Dose–volume correlates. *Int J Radiat Oncol Biol Phys* 2007;67:410–416.
21. Fay M, Tan A, Fisher R, *et al*. Dose–volume histogram analysis as a predictor of radiation pneumonitis in primary lung cancer patients treated with radiotherapy. *Int J Radiat Oncol Biol Phys* 2005;61:1355–1363.
22. Tsujino K, Hirota S, Kotani Y, *et al*. Radiation pneumonitis following concurrent accelerated hyperfractionated radiotherapy and chemotherapy for limited-stage small-cell lung cancer: Dose–volume histogram analysis and comparison with conventional chemoradiation. *Int J Radiat Oncol Biol Phys* 2006;64: 1100–1105.
23. Koh ES, Sun A, Tran TH, *et al*. Clinical dose–volume histogram analysis in predicting radiation pneumonitis in Hodgkin's lymphoma. *Int J Radiat Oncol Biol Phys* 2006;66:223–228.
24. Kwa SL, Lebesque JV, Theuws JC, *et al*. Radiation pneumonitis as a function of mean lung dose: Analysis of pooled data of 540 patients. *Int J Radiat Oncol Biol Phys* 1998;42:1–9.
25. Muller-Runkel R, Vijakumar S. Equivalent total doses for different fractionation schemes, based on the linear-quadratic model. *Radiology* 1991;179:573–577.
26. Mirabell R, Bleher A, Huguenin P, *et al*. Pediatric medulloblastoma: Radiation treatment technique and patterns of failure. *Int J Radiat Oncol Biol Phys* 1997;37:523–539.
27. Sun LM, Yeh SA, Wang CJ, *et al*. Post-operative radiation therapy for medulloblastoma: High recurrence rate in the sub-frontal region. *J Neurooncol* 2002;58:77–85.
28. Carrie C, Alapetite C, Mere P, *et al*., and the French Medulloblastoma Group. Quality control of radiotherapeutic treatment of medulloblastoma in a multi-center study: The contribution of radiotherapy technique to tumor relapse. *Radiother Oncol* 1992;24:71–81.
29. Novakova-Jiresova A, van Luijk P, van Goor H, *et al*. Changes in expression of injury after irradiation of increasing volumes in rat lung. *Int J Radiat Oncol Biol Phys* 2007;67:1510–1518.
30. Claude L, Perol D, Ginestet C, *et al*. A prospective study on radiation pneumonitis following conformal radiation therapy in non-small cell lung cancer: Clinical and dosimetric factors analysis. *Radiother Oncol* 2004;71:175–181.

31. Marks LB, Ma J. Challenges in the clinical application of advanced technologies to reduce radiation-associated normal tissue injury. *Int J Radiat Oncol Biol Phys* 2007;69:4–12.
32. Semenenko V, Molthen R, Li C, *et al*. Irradiation of varying volumes of rat lung to same mean lung dose: A little to a lot or a lot to a little? *Int J Radiat Oncol Biol Phys* 2008;71:838–847.
33. Murshed H, Liu HH, Liao Z, *et al*. Dose and volume reduction for normal lung using intensity-modulated radiotherapy for advanced-stage non-small cell lung cancer. *Int J Radiat Oncol Biol Phys* 2004;58:1258–1267.
34. Cannon GM, Jaradat HA, Rasmussen K, *et al*. Dosimetric evaluation of helical IMRT, traditional IMRT and 3-D conformal radiation for inoperable non-small cell lung cancer. *Int J Radiat Oncol Biol Phys* 2007;69:S632–S633.
35. Wang S, Liao Z, Wei X. Analysis of clinical and dosimetric factors associated with treatment-related pneumonitis (TRP) in patients with non-small cell lung cancer (NSCLC) treated with concurrent chemotherapy and three-dimensional conformal radiotherapy (3D-CRT). *Int J Radiat Oncol Biol Phys* 2006;66: 1399–1407.
36. Arpin D, Perol D, Blay JY, *et al*. Early variations of circulating interleukin-6 and interleukin-10 levels during thoracic radiotherapy are predictive for radiation pneumonitis. *J Clin Oncol* 2005;23:8748–8756.